Measurement of d-C and d-Al total cross sections in the incident momentum range 2.0–4.0 GeV/c

T. Kishida, K. Ishikawa, M. Kuze,* F. Sai,† and S. S. Yamamoto
Department of Physics, University of Tokyo, Tokyo 113, Japan

T. Maki
Department of Physics, University of Occupational and Environmental Health, Kitakyusyu, Fukuoka-ken 807, Japan

I. Arai and A. Manabe
Institute of Physics, Univeristy of Tsukuba, Tsukuba, Ibaraki-ken 305, Japan

H. Koiso and T. Tsuboyama
National Laboratory for High Energy Physics, Tsukuba, Ibaraki-ken 305, Japan
(Received 19 December 1991)

We have made a precise measurement of the d-C total cross sections at 2.0, 2.4, 3.0, and 4.0 GeV/c, and the d-Al total cross sections at 2.0, 3.0, and 4.0 GeV/c. The data were obtained by means of the transmission method covering the momentum transfer squared range of 0.001 to 0.009 $(\text{GeV}/c)^2$ at each momentum. Our results are in good agreement with the Glauber model.

PACS number(s): 25.45.−z, 24.10.Ht

I. INTRODUCTION

There are two different theoretical points of view when considering the scattering of a particle (a single particle such as a nucleon or a composite particle such as nuclei) by a nucleus. One is a macroscopic view, where we consider the nucleus as a single body and treat the process as the scattering by a phenomenological potential. The other is a microscopic view, where we consider the nucleus as the sum of the constituent nucleons and treat the process as multiple scattering between the particle and the nucleons. One of the methods based on the latter view is the multiple-scattering theory called the Glauber model [1,2], which is a standard tool to describe multiple scattering between a nucleon and a nucleus in intermediate energies. Theoretical calculations based on this model have been made and compared with experimental data on a variety of nucleon-nucleus reactions.

When we adopt the latter point of view, the nucleus-nucleus system becomes very important for checking the extension of multiple scattering theories to include a composite projectile. The simplest extension of the nucleon-nucleus collision is d-nucleus scattering, in particular, the d-d scattering. The Glauber-model calculation of the d-d scattering amplitude can be performed rather exactly [3], and d-d total cross sections have been measured [4–7]. The most recent data show that they are in good agreement with the Glauber-model calculations, including the effect of the Fermi motion of the nucleons in the deuteron in the incident-deuteron momentum range of 2.0–4.0 GeV/c [7]. The Glauber-model calculation of other d-nucleus scattering amplitudes can also be performed with the aid of some approximations [8]. But there are very few measurements of d-nucleus total cross sections in the momentum region of 2.0 to 4.0 GeV/c. Only Jaros *et al.* measured the d-He and d-C total cross sections at 3.1 GeV/c [6]. In addition, there is a report of the d-C total cross section which is not a direct measurement but the sum of the d-C elastic, attenuation and stripping total cross sections at 1.69 GeV/c [9,10].

Since high-purity carbon and aluminum targets are readily available, in addition to our d-d total cross-section measurements in the momentum range 1.5–4.0 GeV/c, we have also measured the d-C and d-Al total cross sections in the momentum range 2.0–4.0 GeV/c, and compared the results with Glauber-model calculations. This momentum range is particularly appropriate for such comparison, because the parameters of nucleon-nucleon scattering amplitudes (N-N amplitudes) are strongly dependent on energy. Furthermore, the A dependence of the nucleus-nucleus total cross section for various nuclei at a given incident momentum gives information on the nuclear radius and surface [11]. We have made such a study for d-d, d-C, d-Al at three incident momenta and compared the results with the only other such study by Jaros *et al.* [6].

II. EXPERIMENTAL PROCEDURE

The main part of the experimental arrangement was almost the same as that described in Ref. [7]. A schematic diagram of the detector system is shown in Fig. 1. The data were obtained by means of the transmission method using the secondary beam from an internal target of the 12-GeV proton synchrotron at the National Laboratory for High-Energy Physics (KEK). Since the number of

*Present address: Institute for Nuclear Study, University of Tokyo, Tanashi, Tokyo 188, Japan.
†Present address: IBM Research, Tokyo Research Laboratory, Sanbancho, Chiyoda-ku, Tokyo 102, Japan.

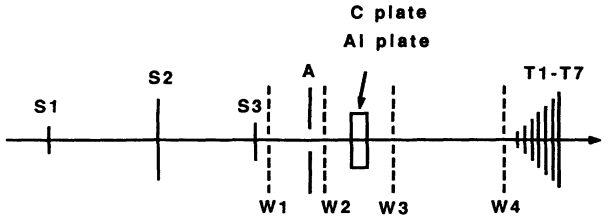

FIG. 1. Schematic diagram of the detector system, which consists of time-of-flight counters $S1$, $S2$, and $S3$, an annular shaped beam defining anticounter A, a transmission counter array $T1-T7$, and four MWPC's $W1-W4$. The targets used in the experiment were a carbon plate and an aluminum plate.

deuterons was 0.5–0.6 % of that of all positively charged particles in this secondary beam, deuterons were selected with a trigger NIM logic by opening a narrow coincidence gate of about 8 ns at the time corresponding to the deuteron time of flight between counters $S1$ and $S3$, which were separated by a distance of 19 m. The trigger logic was $S1\cdot S3\cdot\overline{A}$. Events acquired with this trigger still contained some spurious coincidence signals, which amounted to as much as 40% in the worst case. They were, however, eliminated by using information on the time of flight between counters $S2$ and $S3$ separated by 8.5 m in the off-line analysis. The contamination due to spurious coincidence was reduced to less than 0.1% after this off-line cut. Another source of the contamination was the breakup protons which resulted from the deuterons broken up in the material, but it was estimated to be less than 0.3%. The particles scattered by the target were detected with seven coaxial circular transmission disk counters, which had the diameters of 5.0, 6.5, 8.0, 9.5, 10.5, 12.5, and 15.0 cm. The distance between the target center and the counter array was varied so that at each momentum it covered the momentum transfer squared in the range of $0.001\leq -t\leq 0.009$ $(\mathrm{GeV}/c)^2$. Four multiwire proportional chambers (MWPC's) were used in the off-line analysis for the reconstruction of the incident and scattered particle trajectories. Data from MWPC's $W1$ and $W2$ were used to limit the size of the incident beam within a diameter of 3 cm, and the data from MWPC's $W3$ and $W4$ were used to obtain the acceptances of the seven disk counters.

The only differences between the experimental arrangement in Ref. [7] and this experiment were the targets, the beam momenta, and the numbers of events acquired. The two targets, a carbon plate and an aluminum plate, had almost the same dimensions, which were about 10 cm × 10 cm. The target length (thickness) of the carbon plate was 12.35 ±0.05 mm and that of the aluminum plate was 10.00±0.05 mm. By using the weight and the size of each plate, the number of carbon nuclei per unit area was calculated to be $(1.003\pm0.001)\times10^{-4}$ mb^{-1} and that of aluminum nuclei to be $(5.963\pm0.006)\times10^{-5}$ mb^{-1}. The purity of both targets was better than 99.5%. The measurements were made at the incident deuteron momenta of 2.0, 2.4, 3.0, and 4.0 GeV/c for the carbon target, and 2.0, 3.0, and 4.0 GeV/c for the aluminum target. After all the off-line cuts approximately 450 000 events were obtained with the carbon and aluminum targets and 200 000 events with no target at each momentum.

III. ANALYSIS

By using the data of the transmission-counter hits we calculated the cross section for beam particles to be scattered outside each counter. The cross section for the transmission counter T_i was obtained with the following formula:

$$\sigma_i=-\frac{1}{n}\ln\frac{(N_i/M)_{\mathrm{full}}}{(N_i/M)_{\mathrm{empty}}}\ ,$$

where σ_i is the obtained cross section, n is the number of the target nuclei per unit area, M is the number of incident particles, N_i is the number of particles detected by the transmission counter T_i, and the subscripts "full" and "empty" mean the observables when the target plate was placed at the target point and when no target was placed, respectively. This cross section can also be described by using the differential cross section as follows:

$$\sigma_i=\int_0^{t_{\max}}[1-G_i(t)]\left[\frac{d\sigma}{dt}\right]dt\ ,$$

where $G_i(t)$ is the acceptance function of the transmission counter T_i and $t\equiv|t|$. The acceptance function was defined as the efficiency of a disk counter as a function of t. It was calculated using the information on the hit of each transmission counter and the momentum transfer squared for each event [7]. The latter was obtained with the data from the two beam-defining MWPC's ($W1$ and $W2$) and the two downstream MWPC's ($W3$ and $W4$). By using those acceptance functions the effects of the beam size, the beam divergence, the target length, and position dependence of the efficiency of the transmission counters were correctly taken into account in the correction stage described below.

The cross section σ_i contained the contributions from the Coulomb scattering and the Coulomb-nuclear interference. These contributions were subtracted to obtain the nuclear cross sections. The single Coulomb contribution was given as follows:

$$\int_0^{t_{\max}}[1-G_i(t)]\left[\frac{d\sigma}{dt}\right]_C dt\ ,$$

where $(d\sigma/dt)_C$ is the single Coulomb differential cross section. It was calculated with a screened Coulomb potential. The charge distribution of the electrons of the target atom was treated approximately by using the screening angle χ'_a [12,13], which is momentum dependent and is in the range 0.5×10^{-11}–2.0×10^{-11} for d-C and 0.8×10^{-11}–3.4×10^{-11} for d-Al. The result is

$$\left[\frac{d\sigma}{dt}\right]_C=4\pi\left[\frac{Z\alpha}{\beta}\right]^2\frac{1}{(k^2\chi'^2_a+t)^2}F_d^2(t)F_A^2(t)\ ,$$

where α is the fine-structure constant ($\approx\frac{1}{137}$), Z is the charge of the target nucleus, β and k are the laboratory velocity and momentum of the incident deuteron, respec-

tively, and $F_d(t)$ and $F_A(t)$ are the electric form factor of the deuteron and that of the target nucleus, respectively. The charge distribution of the deuteron was calculated with the wave function obtained by using the Paris potential [14,15]. We assumed the charge distribution of the carbon nucleus to be the same as the distribution predicted by the shell model [16–19] and that of the aluminum nucleus to be the Fermi distribution [16,20,21].

The treatment of multiple Coulomb scattering in the cases of d-C and d-Al was the same as that in the case of d-d [7]. The differential cross section for multiple Coulomb scattering was derived from their angular distributions, which had been calculated by several authors [12,13,22–25]. The probability for the incident particle to be scattered into an angular interval $[\theta,\theta+d\theta]$ is

$$f(\theta)\theta\, d\theta=\eta\, d\eta\left[f_0(\eta)+\frac{1}{B}f_1(\eta)+\frac{1}{B^2}f_2(\eta)+\cdots\right],$$

where

$$f_m(\eta)=\frac{1}{m!}\int_0^\infty u\, du\, J_0(\eta u)\exp(-\tfrac{1}{4}u^2)\times[-\tfrac{1}{4}u^2\ln(\tfrac{1}{4}u^2)]^m .$$

The new variable η is defined as follows [22]:

$$\eta=\frac{\theta}{\chi_c B^{1/2}},$$

where

$$\chi_c^2=\frac{4\pi nZ^2\alpha^2}{k^2\beta^2},$$

and the factor B is momentum dependent and is in the range 12.1–12.6 for d-C and 12.6–13.1 for d-Al [22,23].

The Coulomb-nuclear interference differential cross section, $(d\sigma/dt)_{C\text{-}N\,\mathrm{int}}$ was calculated using the single Coulomb scattering amplitude and the nuclear elastic amplitude. However, at this stage, the nuclear elastic amplitude was not known. We, therefore, calculated this amplitude with the aid of the Glauber model and used an approximation formula [7]. The result is

$$\left[\frac{d\sigma}{dt}\right]_{C\text{-}N\,\mathrm{int}}=-\frac{Z\alpha}{\beta}\sigma_{\mathrm{tot}}\exp(-\tfrac{1}{2}\gamma^2 t)\frac{1}{k^2\chi_\alpha'^2+t}\times F_d(t)F_A(t)[\rho\cos\delta(t)+\sin\delta(t)],$$

where σ_{tot}, ρ, and γ^2 are the nuclear total cross section, the real-to-imaginary ratio, and the slope parameter of d-C or d-Al scattering, respectively, which are predicted by the Glauber model. The phase $\delta(t)$ was calculated with the following formula [26]:

$$\delta(t)=-\frac{Z\alpha}{\beta}\left[\ln\left[\frac{R_d^2}{6}+\frac{R_A^2}{6}\right]t+C\right],$$

where R_d is the root-mean-square radius of the charge distribution of the deuteron, R_A is that of the target nucleus and C is the Euler constant (≈ 0.577).

After subtracting the contributions from the single Coulomb scattering, the multiple Coulomb scattering, and the Coulomb-nuclear interference, we got a set of cross sections due to nuclear interaction only, which we called the corrected cross sections. Because the corrected cross sections were almost linear in t, we were able to obtain the corrected cross sections as functions of t_i, the momentum transfer squared corresponding to the ith counter, which is defined as

$$t_i\equiv\int_0^{t_{\max}} t\left[-\frac{d}{dt}G_i(t)\right]dt .$$

In order to obtain the total cross sections, the corrected cross sections were extrapolated to $t=0$ by fitting them to the form, $\sigma_{\mathrm{tot}}\exp(-At+Bt^2)$, where σ_{tot}, A, and B are free parameters. Figure 2 shows (a) the corrected cross sections of the d-C scattering and (b) those of the d-Al scattering, both at 3.0 GeV/c as examples. The solid curves in the figures are the fitted functions and the filled circles are the corrected cross section. In order to show how large the corrections were, the data before the corrections are also shown as the dotted curves in the figures. The contribution from the Coulomb scattering is comparable to that from the Coulomb-nuclear interference where the momentum transfer squared is around 0.004 $(\mathrm{GeV}/c)^2$ and the former is larger than the latter for $t<0.002$ $(\mathrm{GeV}/c)^2$.

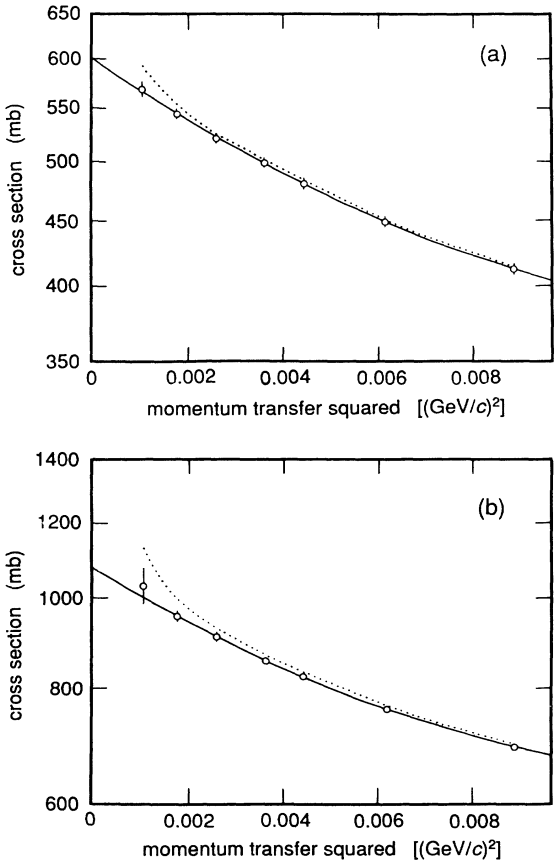

FIG. 2. (a) Corrected cross section data of d-C and (b) those of d-Al at 3.0 GeV/c. The solid curves show the fitted functions and the filled circles are the data. The data before the corrections are also shown as the dotted curves.

TABLE I. Deuteron-carbon total cross sections. The uncertainty in the cross section includes both the statistical and systematic errors.

Momentum (GeV/c)	σ_{tot} (mb)	$\Delta\sigma$ (mb)
2.0	522.4	5.5
2.4	553.1	6.2
3.0	594.2	5.2
4.0	619.0	5.6

TABLE II. Deuteron-aluminum total cross sections. The uncertainty in the cross section includes both the statistical and systematic errors.

Momentum (GeV/c)	σ_{tot} (mb)	$\Delta\sigma$ (mb)
2.0	957	10
3.0	1075	13
4.0	1101	11

IV. RESULTS AND DISCUSSIONS

The d-C total cross sections we obtained are shown in Table I and Fig. 3 as a function of incident momentum, and the d-Al total cross sections are shown in Table II and Fig. 4. The overall errors for d-C and d-Al are about 6 and 10 mb, respectively, which include the statistical errors, systematic errors, and the errors arising from the extrapolation procedure. The statistical errors are about 0.8% for both reactions. Because the counting statistics in each counter is strongly correlated with one another, every covariance between the data of different counters was taken into account in the extrapolation. The systematic errors of the total cross sections are caused mainly by the errors in the correction procedure, and the other effects are negligibly small. The single and multiple Coulomb correction terms are large in the cases of d-C and d-Al as described in the previous chapter, and they are strongly dependent on the form of the acceptance function, because their differential cross sections increase rapidly as the momentum transfer squared approaches zero. We carefully investigated their systematic errors and assumed that the systematic error of multiple Coulomb scattering was 60% and that of single Coulomb scattering was 15% for the smallest counter [7]. They have larger contributions to the overall error than the statistical error in the forward directions, as shown by their error bars in Fig. 2. On the other hand, the error in the Coulomb-nuclear interference term is smaller than the statistical error. We found that the systematic error of the Coulomb-nuclear interference term arises from the uncertainty in the real-to-imaginary ratio calculated with the Glauber model, and estimated this uncertainty to be ± 0.022 for the d-C case and ± 0.017 for the d-Al case. These values come from the uncertainties in the N-N amplitude parameters (see Ref. [7]). We, thus, determined the systematic error of the Coulomb-nuclear interference as $(2.2/\rho)\%$ for the d-C case and $(1.7/\rho)\%$ for the d-Al case, where ρ is the calculated value of the real-to-imaginary ratio. The values of ρ we used are tabulated in Table III. However, some other scattering model might predict different values of ρ from those in Table III. Therefore, we investigated the ρ dependence of the results of the total cross section by changing the values of ρ by ± 0.05 from the values used in our calculation. We found that $(d\sigma_{tot}/d\rho)$ was 62 mb for the d-C case and 190 mb for the d-Al case, and that $(d\sigma_{tot}/d\rho)$ was independent of the incident momentum.

The d-C total cross-section datum by Jaros *et al.* [6] and the sum of the d-C elastic, attenuation, and stripping total cross sections [9,10] are also shown in Fig. 3. Our datum at 3.0 GeV/c is slightly lower than that by Jaros *et al.*, which is the weighted mean of d-C and C-d total cross sections at the same incident momentum per nucleon. Our d-Al total cross-section data are the first result of this reaction in our momentum range.

The calculated values of the cross sections are presented in Figs. 3 and 4 by the dashed and solid curves. The

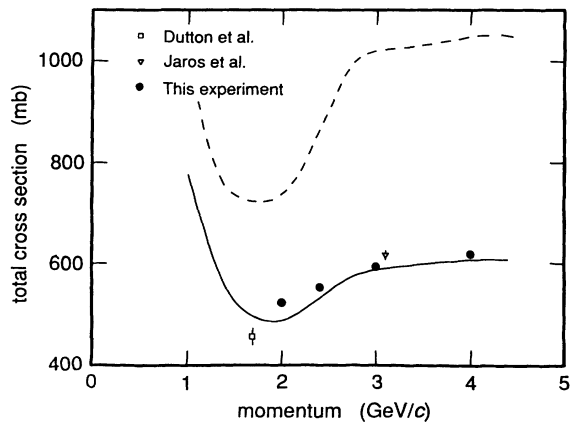

FIG. 3. Deuteron-carbon total cross sections as a function of incident momentum. The dashed curve is the prediction of the impulse approximation, which is equal to 12 $(\sigma_{pp}+\sigma_{np})$ and the solid curve is a Glauber model prediction.

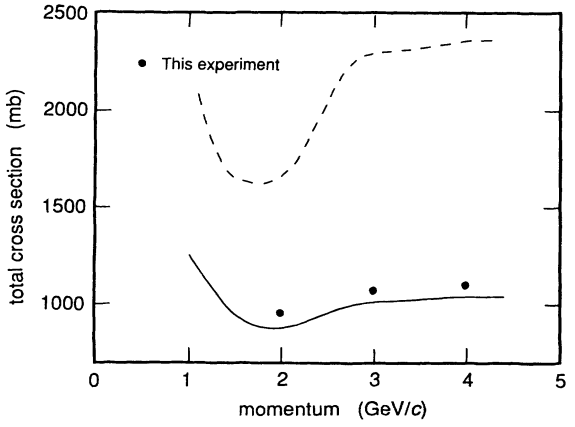

FIG. 4. Deuteron-aluminum total cross sections as a function of incident momentum. The dashed curve is the prediction of the impulse approximation, which is equal to 27$(\sigma_{pp}+\sigma_{np})$ and the solid curve is a Glauber model prediction.

TABLE III. Values of ρ used in the calculation of the Coulomb-nuclear interference correction for d-C and d-Al.

Momentum (GeV/c)	$\rho(d$-C)	$\rho(d$-Al)
2.0	0.156	0.122
2.4	0.071	
3.0	−0.086	−0.065
4.0	−0.158	−0.119

dashed curves represent the impulse approximation: $A(\sigma_{pp}+\sigma_{np})$, which is based on the assumption that the d-nucleus amplitude can be described as the sum of the N-N amplitudes, and the solid curves represent the Glauber-model predictions. The Glauber model is based on the two assumptions described below. The first is that the nucleus-nucleus amplitude and the N-N amplitude can be described with the phase shift $\chi(\mathbf{b})$ as follows:

$$F(\mathbf{q})=\frac{ik}{2\pi}\int \exp(i\mathbf{q}\cdot\mathbf{b})\Gamma(\mathbf{b})d^2\mathbf{b}\ ,$$

$$\Gamma(\mathbf{b})=1-\exp[i\chi(\mathbf{b})]\ ,$$

where $\mathbf{b}$ is the impact parameter vector and $\mathbf{q}$ is the momentum transfer vector. The second assumption is that the phase shift of the nucleus-nucleus scattering can be described as the sum of the phase shifts of the individual nucleon-nucleon scatterings:

$$X_{\rm tot}=\sum_j \chi_j\ ,$$

where $X_{\rm tot}$ is the phase shift of the nucleus-nucleus scattering and χ_j is that of the jth nucleon-nucleon scattering. Consequently, a general form of the d-nucleus elastic scattering amplitude in the case where the target nucleus has A nucleons becomes

$$F_{d\text{-nucl}}(\mathbf{q})=\frac{ik}{2\pi}\int d^2\mathbf{b}\,d^3\mathbf{r}\,d^3\mathbf{r}_1\cdots d^3\mathbf{r}_A \exp(i\mathbf{q}\cdot\mathbf{b})|\Psi_d(\mathbf{r})|^2\,|\Psi_{\rm nucl}(\mathbf{r}_1\cdots\mathbf{r}_A)|^2$$

$$\times\left\langle\left\{1-\prod_{t=1}^{A}[1-\Gamma_a(\mathbf{b}+\mathbf{s}/2-\mathbf{s}_t)][1-\Gamma_b(\mathbf{b}-\mathbf{s}/2-\mathbf{s}_t)]\right\}_T\right\rangle\ ,$$

where $\mathbf{r}$ is the relative coordinate of the nucleon a in the deuteron (the other nucleon is called b), $\mathbf{r}_t$ ($t=1,\ldots,A$) is the internal coordinate of the tth nucleon in the target nucleus, $\Psi_d(\mathbf{r})$ is the configuration space wave function of the deuteron, $\Psi_{\rm nucl}(\mathbf{r}_1\cdots\mathbf{r}_A)$ is that of the target, $\mathbf{s}$ and $\mathbf{s}_t$ are the projections of $\mathbf{r}$ and $\mathbf{r}_t$, respectively, on a plane perpendicular to the incident momentum vector, $\{\ \}_T$ denotes the time-ordering product [3,27], and $\langle\ \rangle$ represents the expectation value of the deuteron and target ground-state spin and isospin wave functions. The exact calculation of the above formula is very tedious, and it is no longer realistic to perform it in general. The main difficulties of the exact calculation originate from the high order of the integration required in the calculation of the amplitude. We therefore calculated the d-nucleus amplitude with some approximations, which were almost the same as those described in Chap. 2 of Ref. [8]. Therefore, in the following we present only the differences between the calculation in Chap. 2 of Ref. [8] and ours. (1) We did not put $\Gamma_{pp}=\Gamma_{np}$, but $\Gamma=(\Gamma_{pp}+\Gamma_{np})/2$. The latter simplification is justified when $|\Gamma_{pp}-\Gamma_{np}|/|\Gamma_{pp}+\Gamma_{np}|$ is relatively small. The functions Γ_{pp} and Γ_{np} were obtained by Fourier transforming the p-p and n-p amplitudes, which were determined using the data from the phase-shift analysis by Arndt, Hyslop, and Roper [28]. (2) We used the deuteron wave function based on the Paris potential [14,15] rather than a Gaussian form. (3) We used the one-body density function of the shell model form [16–19] for the carbon nucleus and that of the Fermi distribution [16,20,21] for the aluminum nucleus.

The agreement between our data and the Glauber-model calculations are rather good for both reactions. The data are slightly larger than the calculations in our momentum range and the differences between them are 1–7 % in the case of d-C, and 6–8 % in the case of d-Al. Though these discrepancies are larger than the accuracies of our experiment, they are not serious, because the calculations would have errors arising from some approximations used [8] and from the uncertainties in the N-N amplitudes and nuclear densities. In particular, the effect of the spin dependence in the Glauber model calculation, which we neglected, might be significant when the multiple scattering terms are large; they are really large enough in the cases of d-C and d-Al, where the cross section defect of d-C is 50–70 % of the total cross section and that of d-Al is 90–130 % of the total cross section. By including the Fermi motion of the nucleons in the nucleus, the agreement between the total cross section data and the Glauber model calculations seems to improve around 2.0 GeV/c in the case of d-C. We, however, did not calculate the effect of Fermi motion because the multiple scattering terms of the Glauber amplitude are large and the refined calculations cannot be carried out as accurately as in the case of the p-d and d-d total cross sections [7].

Finally, we investigated the target dependence of the total cross section. For this purpose, we fitted the d-C and d-Al total cross section data together with our d-d total cross-section data [7] to the formula $\pi r_0^2(2^{1/3}+A^{1/3}-\Delta)^2$ at 2.0, 3.0, and 4.0 GeV/c, where A is the atomic mass number of the target, and r_0 and Δ are related to the nuclear radius and the thickness of the nuclear surface which participates in the interaction only

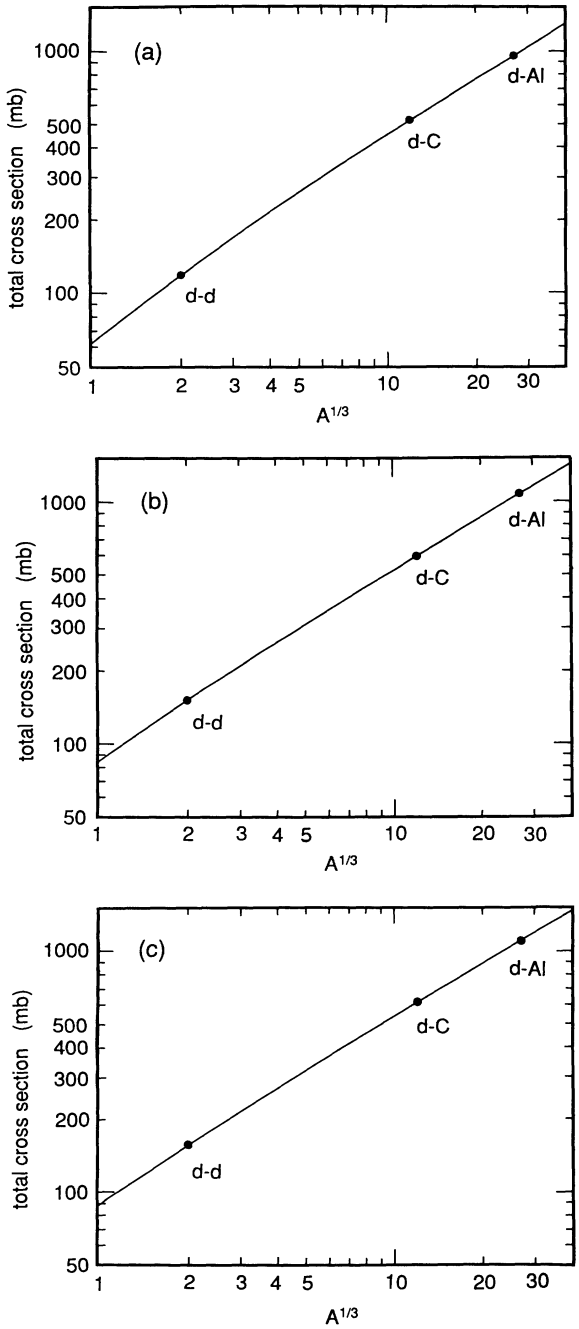

FIG. 5. d-d, d-C, and d-Al total cross sections as a function of the atomic mass number of the target nucleus at (a) 2.0, (b), 3.0, and (c) 4.0 GeV/c.

partially (the partially transparent surface), respectively. They are left as free parameters. Though our data exist only at three points at each momentum, the fits are quite good ($\chi^2=0.07-0.75$ for one degree of freedom) as shown in Fig. 5. The results are as follows:

$r_0=2.06\pm0.01$ fm, $\Delta=1.58\pm0.01$, for 2.0 GeV/c,

$r_0=2.10\pm0.01$ fm, $\Delta=1.47\pm0.01$, for 3.0 GeV/c,

$r_0=2.13\pm0.01$ fm, $\Delta=1.47\pm0.01$, for 4.0 GeV/c.

Our result at 4.0 GeV/c agrees with that by Jaros *et al.*, who obtained $r_0=2.14$ fm and $\Delta=1.48$ from the total cross-section data of d-d, d-α, d-C, α-α, α-C, and C-C at 1.55 and 2.89 GeV/c per nucleon [6]. The good fit of the total cross section data to the above formula reflects the fact that the nucleus is a black sphere, which absorbs the incident wave efficiently, with a radius proportional to $A^{1/3}$ and a partially transparent surface. The effect of the energy dependence of the surface thickness (Δ) is less significant for the total cross section in the case of heavier nuclei, because the fraction of the overlapped surface thickness to the nuclear size becomes smaller. Therefore, the cross section dip around 2.0 GeV/c becomes shallower for heavier targets.

V. CONCLUSIONS

Precise data of the d-C and d-Al total cross sections were obtained in the incident deuteron momentum range of 2.0–4.0 GeV/c. A simple approximation of the Glauber model was successful in explaining our results. However, more sophisticated calculations are needed in order to bring the accuracy of the theoretical calculation to the level of the high accuracy of our experimental data. Some improvements should be made in the future by including the effects of spin dependence, deformation, inelastic intermediate states, etc. For this purpose more complete information on N-N scattering and properties of target nuclei is needed. In addition, our data are also investigated from a macroscopic point of view (e.g., a geometrical consideration). They agree with the prediction based on the assumption that the nucleus is a black sphere which has a volume proportional to the number of the constituent nucleons and an overlapped surface.

ACKNOWLEDGMENTS

We are grateful to the operating crews of the KEK PS, beam channel and cryogenic groups for their assistance during the experiment. We wish to thank Professor T. Nishikawa and the administrative staff of the KEK Physics Department for their assistance and cooperation. We also thank Dr. N. Katayama and Mr. T. Mizusaki for their help and fruitful discussion on the Glauber calculation. The computation for this work was performed at the KEK Computer Center and the Meson Science Laboratory of University of Tokyo.

[1] R. J. Glauber, in *Lectures in Theoretical Physics,* edited by W. E. Brittin and L. G. Dunham (Interscience, New York, 1959), Vol. I, p. 315.
[2] V. Franco and R. J. Glauber, Phys. Rev. **142**, 1195 (1966).
[3] V. Franco, Phys. Rev. **175**, 1376 (1968).
[4] J. Debaisieux, F. Grard, J. Heughebaert, R. Servranckx, and R. Windmolders, Nucl. Phys. **70**, 603 (1965).
[5] A. T. Goshaw, P J. Oddone, M. J. Bazin, and C. R. Sun, Phys. Rev. Lett. **23**, 990 (1969).
[6] J. Jaros *et al.*, Phys. Rev. C **18**, 2273 (1978).
[7] T. Kishida *et al.*, Phys. Rev. C **41**, 180 (1990).
[8] G. Fäldt and H. Pilkuhn, Ann. Phys. (N.Y.) **58**, 454 (1970).
[9] J. D. Jafar, T. J. MacMahon, H. B. van der Raay, D. H. Reading, K. Ruddick, and D.G. Ryan, Nuovo Cimento **48A**, 165 (1967).
[10] L. M. C. Dutton, J. D. Jafar, H. B. van der Raay, D. G. Ryan, J. A. Stiegelmair, R. K. Tandon, and J. F. Reading, Phys. Lett. **16**, 331 (1965).
[11] H. Sato and Y. Okuhara, Phys. Rev. C **34**, 2171 (1986).
[12] H. A. Bethe, Phys. Rev. **89**, 1256 (1953).
[13] A. M. Cormack, Nucl. Phys. **52**, 286 (1964).
[14] M. Lacombe, B. Loiseau, J. M. Richard, R. Vinh Mau, J. Côté, P. Pirés, and R. de Tourreil, Phys. Rev. C **21**, 861 (1980).
[15] M. Lacombe, B. Loiseau, R. Vinh Mau, J. Côté, P. Pirés, and R. de Tourreil, Phys. Lett. **101B**, 139 (1981).
[16] L. R. B. Elton, *Nuclear Sizes* (Oxford University Press, London, 1961), pp. 21–31.
[17] H. A.Bentz, Z. Naturforsch. **24a**, 858 (1969).
[18] H. A. Bentz, Z. Phys. **243**, 138 (1971).
[19] W. Ruckstuhl *et al.*, Phys. Rev. Lett. **49**, 859 (1982).
[20] G. Fey, H. Frank, W. Schütz, and H. Theissen, Z. Phys. **265**, 401 (1973).
[21] J. F. Prewitt and L. E. Wright, Phys. Rev. C **9**, 2033 (1974).
[22] G. Molière, Z. Naturforsch. **3a**, 78 (1948).
[23] U. Fano, Phys. Rev. **93**, 121 (1954).
[24] H. Øverås, CERN Report No. 63-9, 1963.
[25] P. S. Schwaller, B. Favier, D. F. Measday, M. Pepin, P. U. Renberg, and C. Serre, CERN Report No. 72-13, 1972.
[26] M. P. Locher, Nucl. Phys. **B2**, 525 (1967).
[27] R. J. Glauber and V. Franco, Phys. Rev. **156**, 1685 (1967).
[28] R. A. Arndt, J. S. Hyslop III, and L. D. Roper, Phys. Rev. D **35**, 128 (1987).